ARTICLE OPEN

Check for updates

Impact of the valley orbit coupling on exchange gate for spin qubits in silicon

Bilal Tariq[1,2]✉ and Xuedong Hu[1]✉

The mixing of conduction band valleys plays a critical role in determining electronic spectrum and dynamics in a silicon nanostructure. Here, we investigate theoretically how valley–orbit coupling affects the exchange interaction in a silicon double quantum dot. We find that exchange splitting can be strongly suppressed at finite valley phase differences between the dots because of the valley-phase-dependent dressing of the ground states and Coulomb exchange integrals, and a small valley splitting can render the exchange Hamiltonian incomplete in describing low-energy dynamics due to nearby excited valley states. The higher orbital states are also vital in calculating the exchange splitting, which is crucial for applications such as exchange gates for spin qubits.

npj Quantum Information (2022)8:53 ; https://doi.org/10.1038/s41534-022-00554-y

INTRODUCTION

The spin of an electron or a nucleus confined in a semiconductor nanostructure is a qubit with intriguing potential for scalability[1,2]. Out of a multitude of material platforms and encoding schemes[2–10], silicon is particularly enticing as a host for spin qubits because of its low abundance of spinful isotopes, which can be further reduced through isotopic enrichment. As a result, electron spins have particularly long coherence times in Si[11–13]. Furthermore, exchange interaction, which originates from Coulomb interaction and Pauli principle, is inherently strong and allows fast two-spin gates[14–19]. These favorable properties, together with ingenuity from experimentalists, have led to impressive achievements such as high-fidelity single-qubit[20,21] and two-qubit gates[22–25].

A scalable qubit needs to be reproducible in its properties. For electron spin qubits in Si, one of the main concerns has been the valley degree of freedom, i.e., the degeneracy in the Si conduction band, with focus on the valley–orbit coupling induced by the interface, and the associated effects[4,17,26–32]. The study of this problem in single quantum dots have focused on the magnitude of valley splitting and interesting phenomena such as the spin-valley hotspot for spin relaxation[13,33–35]. It has also been recognized in recent years that valley–orbit coupling matrix element is generally complex. Its phase, particularly its variations across neighboring quantum dots, plays a crucial role in determining the tunnel coupling between dots[36–44].

Valley physics in Si has been known to influence exchange splitting strongly, as evidenced by donor pairs in Si[2,17,43,45,46]. With the smooth in-plane confinement of a quantum dot largely removing the strong valley-coupling effect of the hydrogenic donor potential, the nearby interface becomes a crucial factor in determining the remaining valley–orbit coupling. In earlier studies of spin coupling in quantum dots, valley physics was often ignored under the assumption that valley splitting is large[28,47–50], or the valley phase variation is small and can be treated perturbatively[51]. However, our recent study has shown that a single interface step in the wrong place could lead to an almost π phase shift in the valley phase and a strong suppression of the valley splitting[40]. Therefore, there is a critical need to re-examine how electron exchange interaction in a double quantum dot (DQD) depends on valley splitting and valley phase difference.

Here, we study how exchange coupling in a symmetric Si DQD is affected by valley–orbit coupling. We find that the two-electron exchange coupling depends sensitively on the valley phase difference between the dots, and can be strongly suppressed even when valley splitting is large in both dots. If valley splitting is small in at least one of the dots (we will define precisely what we mean by "small"), the exchange gate protocol may have to be re-envisioned altogether because of the presence of additional singlet and triplet states that participate in the low-energy two-electron dynamics. We have also explored the impact on the exchange splitting by the valley–orbit coupling to excited orbital states. Our results clearly demonstrate the challenges posed by the valley–orbit physics on exchange gates for spin qubits in Si, and outline the necessary steps toward reliable exchange gates.

RESULTS

Theoretical model

We calculate the exchange splitting between the ground singlet and triplet states of a symmetric two-electron Si DQD using the configuration interaction (CI) approach. While a DQD in the detuned regime has a tunable exchange splitting[7], it is also well known that effect of charge noise is particularly strong there[52]. We thus mostly restrict ourself to the zero detuning (symmetric) point, where the system is insensitive to the charge noise to the first order[53,54].

The single-electron basis states underlying our two-electron calculations are orthonormalized single-dot envelope functions multiplied by valley eigenstates that contain the local valley–orbit phases,

$$D_{\pm}(\boldsymbol{r}) = D_z(\boldsymbol{r}) \pm e^{-i\phi_D} D_{-z}(\boldsymbol{r}) \quad (1)$$

where $D = \{L, R\}$ denotes the left and right quantum dot. The eigenenergies are $\pm|\Delta_D|$ (the S-orbital energy in the absence of valley–orbit coupling is chosen to be 0), where Δ_D is the valley–orbit couplings. Δ_D is a complex quantity. For an interface

[1]Department of Physics, University at Buffalo, SUNY, Buffalo, NY 14260, USA. [2]National Center for Physics, Quaid-i-Azam University Campus, Islamabad 44000, Pakistan. ✉email: bilaltar@buffalo.edu; xhu@buffalo.edu

with disorder, its magnitude and phase depend on the details of the disorder, as discussed in the Supplementary Materials.

In general exchange splitting in a double dot has two important contributions: electron tunneling that helps lower its kinetic energy, and Coulomb exchange integral. As we demonstrate in the Supplementary Materials, it turns out that both these contributions have the same dependence on the valley phase difference between the dots. In the following we will focus on the tunnel coupling contribution and leave the discussion on the exchange integral to the Supplementary Materials.

We first examine single-electron tunnel couplings in the DQD. With the valley–orbit phase generally different in the two dots, an electron can tunnel between any pair of single-dot states, characterized by the intra- and inter-valley tunnel coupling matrix elements [by "intra" we mean that states in both dots are in the ground (excited) valley eigenstates]:

$$t_{++} = t_{--} = \frac{t_0}{2}\left(1 + e^{-i\phi}\right),\ t_{+-} = t^*_{-+} = \frac{t_0}{2}\left(1 - e^{-i\phi}\right)$$

here, t_0 is the tunnel coupling within the same bulk valleys (z or $-z$). $\phi = \phi_L - \phi_R$ is the valley phase difference in the double dot, with ϕ_L and ϕ_R the valley–orbit phases of the left and right dot, respectively. While the values of ϕ_L and ϕ_R can be calculated, for example using a variational approach[40], it is important to emphasize here that the important quantity in evaluating tunnel coupling between the two dots is the phase difference ϕ. Without loss of generality, we choose $\phi_R = 0$ and ϕ_L as a variable in our exchange energy calculations. In Fig. 1 we plot these two tunneling matrix elements. When $\phi = \phi_L = \phi_R = 0$, valley eigenstates in the two dots are identical, so that tunneling can only happen between the same valleys, i.e., $t_{-+} = 0$. If $\phi = \phi_L = \pi$, the compositions of the valley eigenstates in the two dots are flipped, so that an electron can only tunnel from ground valley eigenstate in one dot to the excited state in the other, or vice versa, i.e., $t_{--} = 0$. This valley phase-dependence by the tunneling matrix elements turns out to be a crucial factor in determining the exchange splitting when we place two electrons in the DQD.

Notice that in a physically realistic situation, both valley phase and valley splitting vary as functions of the interface roughness, such as the location of an interface step, and their variations may be correlated. However, to clarify their individual influences on the exchange splitting, we treat them as independent variables above and for the Hund-Mullikan calculation below.

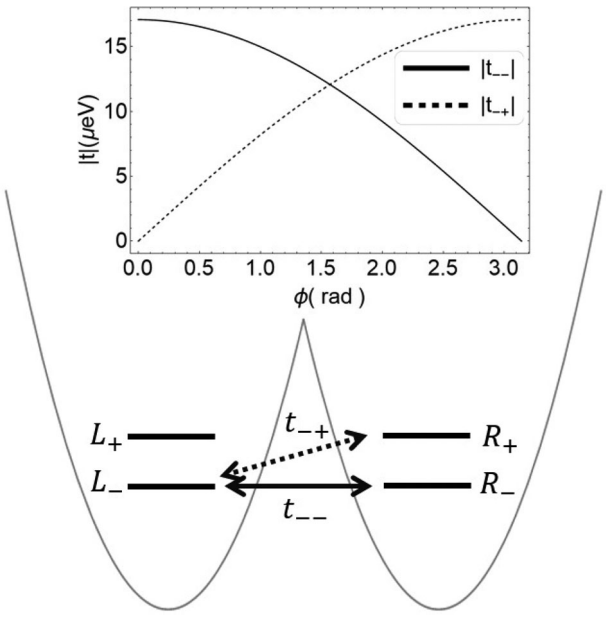

Fig. 1 Electron tunneling in the presence of valleys. Sketch of a double quantum dot with two valley eigenstates in each dot. In the top panel we show the interdot tunnel couplings, both intra- and inter-valley, as a function of the valley phase difference.

Exchange energy within the Hund-Mullikan Model

Accounting for the valley degree of freedom, the minimal CI basis set to calculate the exchange splitting in a Si DQD includes the ground orbital (orthonormalized S orbital of the Fock-Darwin states in the in-plane directions) in each valley for each quantum dot. This is equivalent to a Hund-Mullikan calculation but with two valley eigenstates from each dot, therefore including all the crucial ingredients for an exchange calculation. We will later extend to larger basis sets with up to D-orbitals for each dot in order to validate our results.

From the four orthonormalized single-electron S orbitals in the two dots, one can form 10 symmetric and 6 anti-symmetric two-electron orbital states. Specifically, labeling the S-orbitals in the two dots as L and R, and the valleys as $+$ and $-$ (with valley splittings $2|\Delta_L|$ and $2|\Delta_R|$), we can form four two-dot symmetric or anti-symmetric states: ($L_-R_-, L_-R_+, L_+R_-, L_+R_+$), two single-dot anti-symmetric double occupied states: (L_-L_+, R_-R_+), and six single-dot symmetric double occupied states: ($L_-L_-, L_+L_+, L_-L_+, R_-R_-, R_+R_+, R_-R_+$). We then use these basis states to expand the two-electron Hamiltonian and obtain the singlet and triplet spectrum, respectively. In Fig. 2(a) we show the ground singlet (solid) and triplet (dotted) energies as functions of the interdot valley phase difference $\phi = \phi_L$ ($\phi_R = 0$ is fixed), with the valley splitting in both dots set at 0.1 meV. For a smooth interface, when $\phi_L = \phi_R = 0$, the value of the exchange splitting is at a maximum of 67 neV. This value depends on the tunnel coupling, quantum dot confinement, and coulomb interaction, and can be tuned easily by changing the height of the barrier potential. In this example calculation the dot radius is set at 8 nm (the corresponding orbital excitation energy is 6.3 meV, and the onsite Coulomb energy is 16.1 meV as shown in Table 1) and the interdot distance at 40 nm, making sure that tunnel coupling is quite small.

When both quantum dots have the same valley phase, $\phi = 0$, $t_{--} = t_{++}$ is maximized while $t_{+-} = t_{-+} = 0$. The electrons experience the so-called valley blockade: an electron in $L_\pm$ state can only tunnel to the $R_\pm$ state as they have the same underlying Bloch states, while tunneling between $L_\pm$ and $R_\mp$ are forbidden as their underlying Bloch states are orthogonal. The exchange splitting between the ground singlet and triplet states can thus be calculated within the (L_-L_-, R_-R_-, L_-R_-) block of the block-diagonal Hamiltonian, and the additional valley states do not contribute to the ground singlet-triplet exchange splitting. The situation here is thus the same as the Hund-Mullikan model for a GaAs DQD[14,55].

As the valley phase difference in the double dot increases from zero, valley blockade is lifted. An electron can tunnel between any pair of valley states in the two dots. Consequently, as shown in Fig. 2(a), the exchange splitting decreases, and eventually vanishes when the phase difference reaches π. The physical picture can be most clearly illustrated by comparing panels(c) and (d) of Fig. 2. In Fig. 2(c), where $\phi = \phi_L - \phi_R = 0$, the energy of the ground singlet state is lowered by the dressing from the doubly occupied states L_-L_- and R_-R_-, while the ground triplet cannot be dressed by the doubly occupied states L_-L_+ and R_-R_+ as they are decoupled due to valley blockade between $L_\pm$ and $R_\mp$. As a result a finite energy splitting appears between the ground singlet and triplet states. On the other hand, in Fig. 2(d), where $\phi = \pi$, both ground singlet and triplet states benefit from dressing by the doubly occupied states L_-L_+ and R_-R_+. Doubly occupied states L_-L_- and R_-R_-, which can only be singlet, do not couple to the ground singlet state because of the orthogonality of their underlying Bloch states. As such the ground singlet and triplet states are dressed the same and their energies are lowered equally. Furthermore, as discussed in the

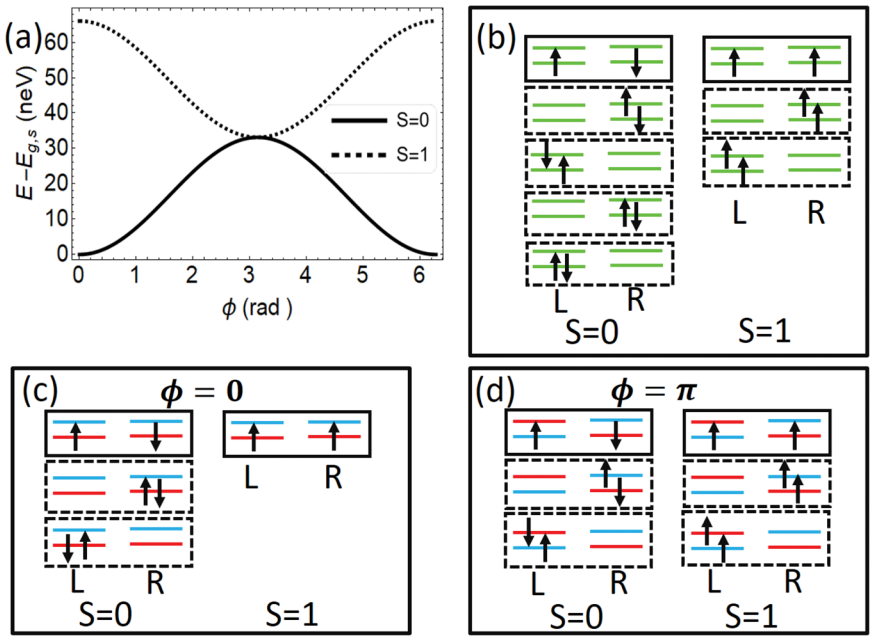

Fig. 2 Exchange splitting calculated with only single-dot s-orbitals. a Dependence of the ground singlet ($S = 0$) and triplet ($S = 1$) energy levels on the valley phase difference between the two dots (with $\phi_R = 0$). For a smooth interface, the exchange interaction is $E_J = 67$ neV with $|\Delta_L| = |\Delta_R| = 0.1$ meV for the chosen double dot parameters. **b** shows the states of ground singlet and triplet for a general ϕ. Panels **c** and **d** illustrates state dressing for phase difference $\phi = 0$ and $\phi = \pi$, respectively. The ground singlet energy level ($E_{g,s}$) for smooth interface is the zero energy reference.

Table 1. Relevant Coulomb matrix elements for two electrons in a double quantum dot, which show a clear hierarchy in their magnitudes.

Coulomb terms	Coulomb expression	Values
On-site	$u = \langle L_-(\boldsymbol{r}_1)L_-(\boldsymbol{r}_2)\|H_C\|L_-(\boldsymbol{r}_1)L_-(\boldsymbol{r}_2)\rangle$	16.1 meV
Interdot	$k = \langle L_-(\boldsymbol{r}_1)R_-(\boldsymbol{r}_2)\|H_C\|L_-(\boldsymbol{r}_1)R_-(\boldsymbol{r}_2)\rangle$	3.1 meV
Overlap	$s = \|\langle L_-(\boldsymbol{r}_1)L_-(\boldsymbol{r}_2)\|H_C\|L_-(\boldsymbol{r}_1)R_-(\boldsymbol{r}_2)\rangle\|$	− 5.7 μeV
Exchange	$j = \|\langle L_-(\boldsymbol{r}_1)R_-(\boldsymbol{r}_2)\|H_C\|R_-(\boldsymbol{r}_1)L_-(\boldsymbol{r}_2)\rangle\|$	46.3 neV

Supplemental Materials, the Coulomb exchange also has a dependence on the valley phase difference in the form of $\cos^2(\phi)$. Including both these contributions, the exchange splitting decreases as ϕ increases from 0, and vanishes at $\phi = \pi$.

In short, our results here show that exchange splitting in a Si double quantum dot can be significantly impacted by the valley phase difference between the two dots, and can be completely suppressed if $\phi = \pi$. To make an exchange gate operable, it is important to avoid such operation points. In the context of interface step that we consider below, one could conceivably shift away from these unfavorable points by shifting the quantum dots relative to each other using top gate potentials, then tune the value of exchange energy by varying the tunnel barrier height as long as $\phi \neq \pi$.

The results of Fig. 2 are obtained with finite valley splittings of 0.1 meV in each dot. In other words, valley phase difference between the two dots plays a pivotal role in determining the exchange splitting even in the presence of finite valley splittings, making our results meaningful for both SiGe and SiMOS quantum dots.

Effects of valley splitting on exchange coupling

The magnitude of the S-orbital valley–orbit coupling determines the ground state valley splitting in a Si quantum dot, ranging from a few hundreds of μeV[33,35,37] to less than 10 μeV[13,36,44,56]. If the valley splitting is small compared with the thermal broadening of a nearby reservoir (at a typical electron temperature of 150 mK,

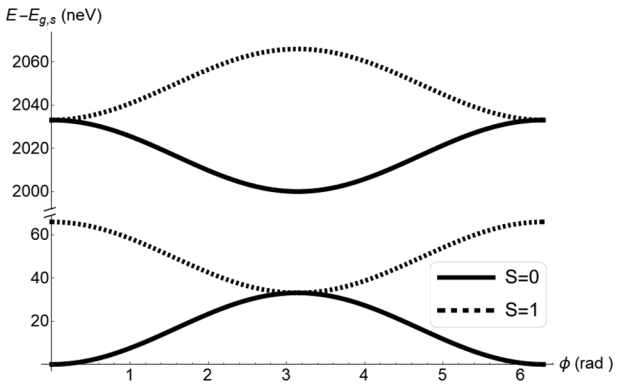

Fig. 3 Low-energy spectrum of a two-electron Si DQD. Energy levels of the ground and first excited singlet ($S = 0$) and triplet states ($S = 1$) in a Si double dot as a function of the interdot valley phase difference ϕ. For this calculation we choose $\Delta_R = 1$ μeV, $\Delta_L = 100$ μeV, and $\phi_R = 0$.

the thermal broadening is about 10 μeV) for spin initialization, an electron could be initialized into the correct spin state but with a mixed valley state. Such an unwanted orbital freedom may not affect single spin manipulation, assuming the two valley eigenstates having the same g-factor. However, when considering two-spin exchange coupling, this additional freedom in valley occupation could lead to significant difficulties.

Consider a situation when the valley–orbit coupling in the right dot is two orders of magnitude smaller than in the left dot: $|\Delta_L| = 100$ μeV and $|\Delta_R| = 1$ μeV. In Fig. 3 we plot the energies of the ground and first excited singlet and triplet states as functions of the valley phase difference. The ground states have the same behavior as in Fig. 2, as expected. The first excited singlet and triplet states are roughly 2 μeV above the ground singlet and triplet states, respectively, with the electron in the right dot occupying the excited valley state, i.e., L_-R_+. Notice that the phase-dependence of the excited singlet and triplet states are

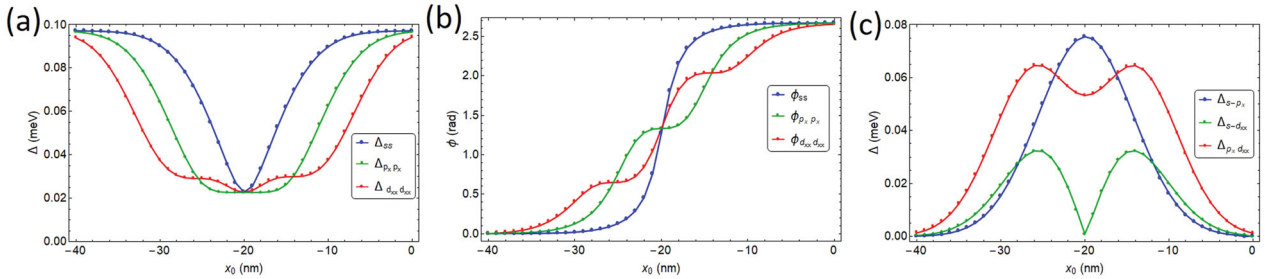

Fig. 4 Valley–orbit couplings as functions of the interface step position. Valley–orbit coupling as a function of the location of a single interface step. **a** and **b** present the magnitudes and phases of the diagonal valley–orbital coupling elements in Eq. (2), respectively, while **c** shows the magnitude of the off-diagonal terms of the valley–orbit coupling matrix of Eq. (2).

quite different from the respective ground state. If an electron is initialized into the right dot in a superposition of the valley eigenstates $(\alpha|R_-\rangle + \beta|R_+\rangle)|\uparrow\rangle$, when tunnel coupling is allowed, the respective singlet-triplet states that can be formed from $|R_-\rangle$ and $|R_+\rangle$, i.e., the ground and first excited singlet-triplet pairs we plot in Fig. 3, will in general have different singlet-triplet splittings. Consequently, the phase accumulated during an exchange gate will be different in these two pairs, making a spin swap gate almost impossible[1].

In short, a necessary condition for exchange gate protocol to be valid in a Si DQD is that the valley splitting in each dot is much larger than the thermal broadening of the reservoir used for initialization. This condition guarantees a high-fidelity preparation for a spin qubit in the ground valley eigenstate, taking away any uncertainty in the follow-up spin manipulations.

When $|\Delta_R|$ (and/or $|\Delta_L|$) is further reduced, the ground and excited singlet and triplet states for the DQD become even more compact in the energy spectrum, and their dynamics cannot be straightforwardly disentangled, as we discuss in the Supplemental Materials. While the physics at this limit is subtle and interesting, the DQD does not have any utility for spin qubit manipulation anymore as the system cannot be properly initialized and controlled.

Exchange energy in the presence of an interface step

In the model calculations above we vary either the valley phase difference or the valley splittings in a quantum dot as an independent variable. In a realistic situation, however, both would depend on the properties of the interface. As such they tend to change in a correlated manner, as has been illustrated in Si/SiGe heterostructures with a single atomic layer step at the interface inside a quantum dot[28,37,40,41,57,58]. Here, we calculate the exchange splitting in a Si DQD in the presence of an interface step. To go beyond the qualitative discussions within the Hund-Mullikan model above, we also include higher-energy orbital states in our CI calculation.

Before delving into the two-electron calculations, we need to first calculate the valley–orbit matrix elements among all the single-electron orbitals. This would allow us to better clarify the effects of the higher orbital states and the valley–orbit coupling parameters on the ground state exchange splitting. Including the s-, p-, and d-orbitals (corresponding to six orbitals per pot) for the in-plane wave function in each dot, the different valley–orbit coupling terms can be summarized in a matrix as

$$\Delta = \begin{pmatrix} \Delta_{ss} & \Delta_{sp_x} & 0 & \Delta_{sd_{xx}} & 0 & 0 \\ \Delta_{p_x s} & \Delta_{p_x p_x} & 0 & \Delta_{p_x d_{xx}} & 0 & 0 \\ 0 & 0 & \Delta_{p_y p_y} & 0 & 0 & 0 \\ \Delta_{d_{xx} s} & \Delta_{d_{xx} p_x} & 0 & \Delta_{d_{xx} d_{xx}} & 0 & 0 \\ 0 & 0 & 0 & 0 & \Delta_{d_{xy} d_{xy}} & 0 \\ 0 & 0 & 0 & 0 & 0 & \Delta_{d_{yy} d_{yy}} \end{pmatrix}. \quad (2)$$

The terms in Δ generally vary differently with the step position as the orbitals have different forms. Given a step position and orientation, each of the matrix elements can be calculated straightforwardly. The Δ matrix can then be included when calculating the orthonormal single-electron eigenbasis, over which we construct the two-electron states and calculate the exchange splitting.

In Fig. 4 (a), we show the step-position dependence of the magnitude of the valley–orbit coupling (valley splittings for the particular orbitals) in the diagonal elements of the left quantum dot with a monolayer step. The step considered here is along the *y* direction and can thus be identified by its position along the *x*-axis. Note that the influence of the step on the diagonal elements $\Delta_{p_y p_y}$ and $\Delta_{d_{yy} d_{yy}}$ are the same as on Δ_{ss} as these orbitals share the same form along the *x*-axis. For the same reason, $\Delta_{p_x p_x} = \Delta_{d_{xy} d_{xy}}$. Similar to the ground orbital state, the valley splittings for the other orbital states are also reduced when the step cuts through the quantum dot, reaching their minima when the step is located at the center of the dot. Furthermore, the valley–orbit coupling behavior is not the same for different orbital states due to the shape of the Fock-Darwin wave functions along the *x* direction.

Valley phases for each orbital state also depend on the step location, as shown in Fig. 4(b), varying from 0 to 0.85π. The change in the valley phase of $\phi_{d_{xx} d_{xx}}$ is wider with two stairs like features, because of the presence of three nodes in the *x* direction in the d_{xx} orbital. On the other hand, $\phi_{p_x p_x} = \phi_{d_{xy} d_{xy}}$, with one node present in their wave functions along the *x* direction. Lastly, ϕ_{ss} changes the most sharply as the s-orbital is the smallest.

With multiple orbitals from each dot, new off-diagonal valley–orbit coupling terms also appear. In this paper, we consider up to the d-orbital states in our calculations, which leads to three non-vanishing off-diagonal terms, Δ_{sp_x}, $\Delta_{p_x d_{xx}}$ and $\Delta_{sd_{xx}}$. In Fig. 4 we show how the position of the step affects the magnitude of each of these off-diagonal terms. In particular, the magnitude of Δ_{sp_x} reaches a maximum value of ~ 0.075 meV when the step is at the center of the dot. $\Delta_{p_x d_{xx}}$ and $\Delta_{sd_{xx}}$ are also finite. The phases of these off-diagonal terms do not have much of an effect on our exchange calculation and hence have not been shown here. As our results below indicate, these finite off-diagonal elements in the valley–orbit coupling matrix is quite important in our calculation of the ground state exchange splitting.

With all the single-electron orbitals clarified, CI calculations for two electrons in the DQD can be performed. In Fig. 5 we plot the ground state exchange splitting as a function of the step location x_0, with the step oriented perpendicular to the interdot axis. $x_0 = 0$ refers to the situation when the step is at the midpoint between the two dots, and $x_0 = -20$ nm is when the step passes through the middle of the left dot. The most important feature in this figure is the suppression of exchange coupling when the step is located in between the two dots, similar to what we find in Fig. 2 (a) when we only consider the s-orbitals. This suppression has the same origin as well: when the step is in between the dots (at or near $x_0 = 0$), the valley phase difference between the dots

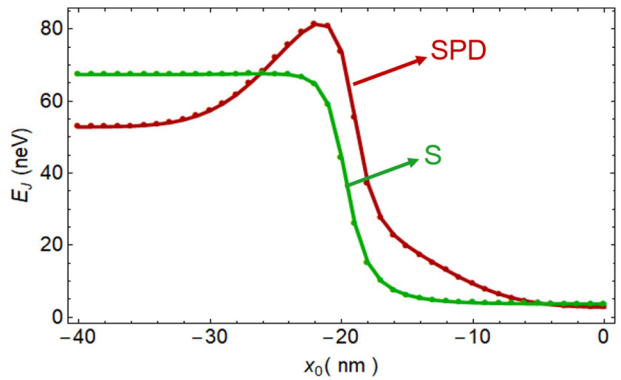

Fig. 5 Exchange splitting as a function of the interface step location. Two-electron exchange interaction as a function of the interface atomic step position, with different CI basis sets (*s* only, or with *spd* orbital states). The center of the DQD lies at the origin $x_0 = 0$. The center of the left dot is at $x_0 = -20$ nm, and the dot radius is $\ell_0 = 8$ nm.

is ~ 0.85π, making the tunnel coupling between the ground valley states in the two dots very small and the exchange coupling strongly suppressed.

There are two interesting features in Fig. 5 due to higher orbitals. There is a broad peak when the step is in the middle of the left dot, and there is a longer tail of finite exchange splitting (as compared to the s-orbital only calculation) as the step approaches the middle between the dots. These features are mainly the results of a competition between two influences: the phase of the Δ_{ss}, and the magnitude of Δ_{sp_x}. As discussed for Fig. 2, a non-vanishing phase for Δ_{ss} suppresses the magnitude of the exchange splitting for the ground singlet-triplet pair. The term Δ_{sp_x} originates from the symmetry breaking within the left dot due to the presence of the step. It reaches its maximum magnitude when the step is at the center of the dot, and causes a linear change in the exchange splitting (see Supplement Materials). The valley–orbit coupling in the excited states plays an important role here because we have two small quantum dots, such that orbital excitation energy (~6.3 meV) is much smaller than the onsite Coulomb interaction ~16 meV, making the dressing of the ground singlet and triplet states by the orbital excited states as important as the doubly occupied ground orbital states. In other words, to achieve numerical convergence for an exchange calculation, more orbital states need to be included. However, for the purpose of exploring the qualitative effects of the valley–orbit coupling, our finite-size calculation here is sufficient.

DISCUSSIONS AND CONCLUSIONS

Our calculations above are for a symmetric Si double quantum dot. Nevertheless, the lessons we have learned are applicable to the finite-detuning regime, where exchange splitting is dominated by the tunnel coupling between the (11) singlet and (02) [or (20)] ground singlet state [here (11) and (02) refer to the electron occupation in each dot][7,48]. This tunnel coupling is again sensitively dependent on the interdot valley phase difference. For example, a π phase shift would render the ground singlet-singlet anti-crossing a crossing, with a vanishing exchange splitting between ground singlet and triplet states. Meanwhile, a reduction in the magnitude of the valley splitting would push all the (11) and (02) crossings and anti-crossings close to each other, making exchange control more difficult to achieve[48]. In short, valley–orbit coupling plays as important a role in the detuned regime as for a symmetric Si DQD. Further explorations are needed to firmly establish the viability and conditions for exchange gates in this regime.

In our study here we take the interdot valley-phase difference ϕ as a well-defined quantity and possibly tunable by external field. Such a model is applicable in situations where effective mass model is appropriate, such as an interface between Si and SiGe with interface steps but otherwise smooth and sharp. Another main source of interface roughness that affects valley–orbit coupling is the atomistic-scale alloy disorder near the interface, whether in a Si/SiGe or Si/SiO_2 system[59,60]. Exchange interaction in such a system would certainly be affected. However, the behavior of valley–orbit phase, which is a well-defined concept only within the effective mass model, in a system with roughness of very small length scale is unknown. For disorders at such length-scale, an atomistic approach such as the tight binding approximation would be more appropriate than the effective mass approximation. Consequently one may calculate the single-electron tunnel coupling and two-electron exchange coupling directly, and calculate the corresponding effective valley–orbit coupling (both magnitude and phase) afterward.

In conclusion, we have performed analytical and numerical analysis of the ground singlet-triplet exchange splitting of a symmetric Si double quantum dot. Our results show that valley–orbit coupling in the two dots play crucial roles in determining the exchange energy. In particular, it depends sensitively on the valley phase difference between the two dots, reaching a minimum when the phase difference is π, even in the presence of large valley splittings in both dots. We also show that it is imperative that valley splitting in each of the quantum dots should be large compared to the thermal broadening of the reservoir, such that a spin qubit can be properly initialized. By examining the splitting in both the ground and first excited singlet-triplet pairs, we show that exchange gate would not work properly if both of these manifolds are involved in the spin dynamics. Lastly, we show that the higher-energy orbital states also make important contributions in determining the value of the exchange energy, particularly for smaller dots with large on-site Coulomb interaction.

While our results are particularly relevant for Si/SiGe quantum dots, the phase-dependence by the exchange coupling, irrespective of the magnitude of the valley splitting, is an important observation for SiMOS quantum dots as well, which tend to have larger valley splittings but also have an amorphous interface. Our results shine a further spotlight on the interface roughness, and the need to understand and characterize them in order to achieve scalable quantum computing based on spin qubits in silicon.

DATA AVAILABILITY

The data that support the findings of this study are available from the corresponding author upon reasonable request.

CODE AVAILABILITY

The code that support the findings of this study are available from the corresponding author upon reasonable request.

Received: 10 November 2021; Accepted: 24 March 2022;
Published online: 10 May 2022

REFERENCES

1. Loss, D. & DiVincenzo, D. P. Quantum computation with quantum dots. *Phys. Rev. A* **57**, 120 (1998).
2. Kane, B. E. A silicon-based nuclear spin quantum computer. *Nature* **393**, 133–137 (1998).
3. Hanson, R., Kouwenhoven, L. P., Petta, J. R., Tarucha, S. & Vandersypen, L. M. Spins in few-electron quantum dots. *Rev. Mod. Phys.* **79**, 1217 (2007).
4. Zwanenburg, F. A. et al. Silicon quantum electronics. *Rev. Mod. Phys.* **85**, 961 (2013).

5. Borselli, M. G. et al. Pauli spin blockade in undoped si/sige two-electron double quantum dots. *Appl. Phys. Lett.* **99**, 063109 (2011).
6. DiVincenzo, D. P., Bacon, D., Kempe, J., Burkard, G. & Whaley, K. B. Universal quantum computation with the exchange interaction. *Nature* **408**, 339–342 (2000).
7. Petta, J. R. et al. Coherent manipulation of coupled electron spins in semiconductor quantum dots. *Science* **309**, 2180–2184 (2005).
8. Shi, Z. et al. Fast hybrid silicon double-quantum-dot qubit. *Phys. Rev. Lett.* **108**, 140503 (2012).
9. Benito, M. & Burkard, G. Hybrid superconductor-semiconductor systems for quantum technology. *Appl. Phys. Lett.* **116**, 190502 (2020).
10. Hendrickx, N., Franke, D., Sammak, A., Scappucci, G. & Veldhorst, M. Fast two-qubit logic with holes in germanium. *Nature* **577**, 487–491 (2020).
11. Veldhorst, M. et al. An addressable quantum dot qubit with fault-tolerant control-fidelity. *Nat. Nanotechnol.* **9**, 981 (2014).
12. Muhonen, J. T. et al. Storing quantum information for 30 seconds in a nanoelectronic device. *Nat. Nanotechnol.* **9**, 986–991 (2014).
13. Borjans, F., Zajac, D., Hazard, T. & Petta, J. Single-spin relaxation in a synthetic spin-orbit field. *Phys. Rev. Appl.* **11**, 044063 (2019).
14. Burkard, G., Loss, D. & DiVincenzo, D. P. Coupled quantum dots as quantum gates. *Phys. Rev. B* **59**, 2070 (1999).
15. Hu, X. & Sarma, S. D. Spin-based quantum computation in multielectron quantum dots. *Phys. Rev. A* **64**, 042312 (2001).
16. Burkard, G. & Loss, D. Cancellation of spin-orbit effects in quantum gates based on the exchange coupling in quantum dots. *Phys. Rev. Lett.* **88**, 047903 (2002).
17. Koiller, B., Hu, X. & Sarma, S. D. Exchange in silicon-based quantum computer architecture. *Phys. Rev. Lett.* **88**, 027903 (2001).
18. Harvey-Collard, P. et al. Coherent coupling between a quantum dot and a donor in silicon. *Nat. Commun.* **8**, 1–6 (2017).
19. Yang, X.-C. & Wang, X. Suppression of charge noise using barrier control of a singlet-triplet qubit. *Phys. Rev. A* **96**, 012318 (2017).
20. Yoneda, J. et al. A quantum-dot spin qubit with coherence limited by charge noise and fidelity higher than 99.9%. *Nat. Nanotechnol.* **13**, 102–106 (2018).
21. Yang, C. et al. Silicon qubit fidelities approaching incoherent noise limits via pulse engineering. *Nat. Electron.* **2**, 151–158 (2019).
22. Sigillito, A., Gullans, M., Edge, L., Borselli, M. & Petta, J. Coherent transfer of quantum information in a silicon double quantum dot using resonant swap gates. *NPJ Quantum Inf.* **5**, 1–7 (2019).
23. Veldhorst, M. et al. A two-qubit logic gate in silicon. *Nature* **526**, 410–414 (2015).
24. Watson, T. et al. A programmable two-qubit quantum processor in silicon. *Nature* **555**, 633–637 (2018).
25. Chan, K. W. et al. Exchange coupling in a linear chain of three quantum-dot spin qubits in silicon. *Nano Lett.* **21**, 1517–1522 (2021).
26. Hada, Y. & Eto, M. Exchange coupling in silicon double quantum dots. *Jpn. J. Appl. Phys.* **43**, 7329 (2004).
27. Friesen, M., Eriksson, M. & Coppersmith, S. Magnetic field dependence of valley splitting in realistic si/ si ge quantum wells. *Appl. Phys. Lett.* **89**, 202106 (2006).
28. Friesen, M., Chutia, S., Tahan, C. & Coppersmith, S. Valley splitting theory of si ge/ si/ si ge quantum wells. *Phys. Rev. B* **75**, 115318 (2007).
29. Goswami, S. et al. Controllable valley splitting in silicon quantum devices. *Nat. Phys.* **3**, 41–45 (2007).
30. Shi, Z. Spin and charge qubits in siliconsilicon germanium quantum dots. Ph.D. thesis (The University of Wisconsin-Madison, 2013).
31. Benito, M., Petta, J. R. & Burkard, G. Optimized cavity-mediated dispersive two-qubit gates between spin qubits. *Phys. Rev. B* **100**, 081412 (2019).
32. Huang, P. & Hu, X. Electric-dipole-induced resonance and decoherence of a dressed spin in a quantum dot. Preprint at https://arxiv.org/abs/2103.05817 (2021).
33. Yang, C. et al. Spin-valley lifetimes in a silicon quantum dot with tunable valley splitting. *Nat. Commun.* **4**, 1–8 (2013).
34. Huang, P. & Hu, X. Spin relaxation in a si quantum dot due to spin-valley mixing. *Phys. Rev. B* **90**, 235315 (2014).
35. Hollmann, A. et al. Large, tunable valley splitting and single-spin relaxation mechanisms in a si/si x ge 1- x quantum dot. *Phys. Rev. Appl.* **13**, 034068 (2020).
36. Burkard, G. & Petta, J. R. Dispersive readout of valley splittings in cavity-coupled silicon quantum dots. *Phys. Rev. B* **94**, 195305 (2016).
37. Gamble, J. K. et al. Valley splitting of single-electron si mos quantum dots. *Appl. Phys. Lett.* **109**, 253101 (2016).
38. Zhao, X. & Hu, X. Coherent electron transport in silicon quantum dots. Preprint at https://arxiv.org/abs/1803.00749 (2018).
39. Tagliaferri, M. et al. Impact of valley phase and splitting on readout of silicon spin qubits. *Phys. Rev. B* **97**, 245412 (2018).
40. Tariq, B. & Hu, X. Effects of interface steps on the valley-orbit coupling in a si/sige quantum dot. *Phys. Rev. B* **100**, 125309 (2019).
41. Ferdous, R. et al. Valley dependent anisotropic spin splitting in silicon quantum dots. *NPJ Quantum Inf.* **4**, 1–8 (2018).
42. Hosseinkhani, A. & Burkard, G. Electromagnetic control of valley splitting in ideal and disordered si quantum dots. *Phys. Rev. Res.* **2**, 043180 (2020).
43. Voisin, B. et al. Valley interference and spin exchange at the atomic scale in silicon. *Nat. Commun.* **11**, 1–11 (2020).
44. Borjans, F. et al. Probing the variation of the intervalley tunnel coupling in a silicon triple quantum dot. *PRX Quantum* **2**, 020309 (2021).
45. Hollenberg, L., Greentree, A., Fowler, A. & Wellard, C. Two-dimensional architectures for donor-based quantum computing. *Phys. Rev. B* **74**, 045311 (2006).
46. Salfi, J. et al. Spatially resolving valley quantum interference of a donor in silicon. *Nat. Mater.* **13**, 605–610 (2014).
47. Li, Q., Cywiński, Ł., Culcer, D., Hu, X. & Sarma, S. D. Exchange coupling in silicon quantum dots: theoretical considerations for quantum computation. *Phys. Rev. B* **81**, 085313 (2010).
48. Culcer, D., Cywiński, Ł., Li, Q., Hu, X. & Sarma, S. D. Quantum dot spin qubits in silicon: multivalley physics. *Phys. Rev. B* **82**, 155312 (2010).
49. Culcer, D., Hu, X. & Sarma, S. D. Interface roughness, valley-orbit coupling, and valley manipulation in quantum dots. *Phys. Rev. B* **82**, 205315 (2010).
50. Friesen, M. & Coppersmith, S. Theory of valley-orbit coupling in a si/sige quantum dot. *Phys. Rev. B* **81**, 115324 (2010).
51. Culcer, D., Saraiva, A., Koiller, B., Hu, X. & Sarma, S. D. Valley-based noise-resistant quantum computation using si quantum dots. *Phys. Rev. Lett.* **108**, 126804 (2012).
52. Shulman, M. D. et al. Demonstration of entanglement of electrostatically coupled singlet-triplet qubits. *Science* **336**, 202–205 (2012).
53. Reed, M. et al. Reduced sensitivity to charge noise in semiconductor spin qubits via symmetric operation. *Phys. Rev. Lett.* **116**, 110402 (2016).
54. Martins, F. et al. Noise suppression using symmetric exchange gates in spin qubits. *Phys. Rev. Lett.* **116**, 116801 (2016).
55. Hu, X. & Sarma, S. D. Hilbert-space structure of a solid-state quantum computer: two-electron states of a double-quantum-dot artificial molecule. *Phys. Rev. A* **61**, 062301 (2000).
56. Zajac, D., Hazard, T., Mi, X., Wang, K. & Petta, J. R. A reconfigurable gate architecture for si/sige quantum dots. *Appl. Phys. Lett.* **106**, 223507 (2015).
57. Gamble, J. K., Eriksson, M., Coppersmith, S. & Friesen, M. Disorder-induced valley-orbit hybrid states in si quantum dots. *Phys. Rev. B* **88**, 035310 (2013).
58. Zimmerman, N. M., Huang, P. & Culcer, D. Valley phase and voltage control of coherent manipulation in si quantum dots. *Nano Lett.* **17**, 4461–4465 (2017).
59. Grange, T. et al. Atomic-scale insights into semiconductor heterostructures: from experimental three-dimensional analysis of the interface to a generalized theory of interfacial roughness scattering. *Phys. Rev. Appl.* **13**, 044062 (2020).
60. Wuetz, B. P. et al. Atomic fluctuations lifting the energy degeneracy in si/sige quantum dots. Preprint at https://arxiv.org/abs/2112.09606 (2021).

ACKNOWLEDGEMENTS

We thank support by US ARO through grant W911NF1710257.

AUTHOR CONTRIBUTIONS

B.T. performed derivation and numerical calculation. B.T. and X.H. researched, analyzed, and prepared the manuscript.

COMPETING INTERESTS

The authors declare no competing interests.

ADDITIONAL INFORMATION

Supplementary information The online version contains supplementary material available at https://doi.org/10.1038/s41534-022-00554-y.

Correspondence and requests for materials should be addressed to Bilal Tariq or Xuedong Hu.

Reprints and permission information is available at http://www.nature.com/reprints

Publisher's note Springer Nature remains neutral with regard to jurisdictional claims in published maps and institutional affiliations.